

# Imaging LIDARs for Space Applications

J. Pereira do Carmo<sup>a</sup>, B. Moebius<sup>b</sup>, M. Pfennigbauer<sup>c</sup>, R. Bond<sup>d</sup>, I. Bakalski<sup>e</sup>, M. Foster<sup>f</sup>, S. Bellis<sup>g</sup>,  
M. Humphries<sup>h</sup>, R. Fisackerly<sup>a</sup>, B. Houdou<sup>a</sup>

<sup>a</sup>European Space Agency, ESTEC Keplerlaan 1, 2200AG Noordwijk, The Netherlands  
([joao.pereira.do.carmo@esa.int](mailto:joao.pereira.do.carmo@esa.int), [richard.fisackerly@esa.int](mailto:richard.fisackerly@esa.int), [berengere.houdou@esa.int](mailto:berengere.houdou@esa.int));

<sup>b</sup>Jena-Optronik GmbH, Pruessingstr. 41, D-07745 Jena, Germany  
([bettina.moebius@jena-optronik.de](mailto:bettina.moebius@jena-optronik.de))

<sup>c</sup>RIEGL Research, Riedenburgstr.48 A-3580 Horn, Austria  
([martin.pfennigbauer@rieglresearch.com](mailto:martin.pfennigbauer@rieglresearch.com))

<sup>d</sup>ABSL Space Products, Culham Science Centre, Abingdon, Oxon, OX14 3ED, UK  
([robert.bond@absinspaceproducts.com](mailto:robert.bond@absinspaceproducts.com))

<sup>e</sup>LIDAR Technologies Inc, 10 Gerard Ave., Ste.202, Timonium, MD 21093, USA,  
([lidartech@verizon.net](mailto:lidartech@verizon.net))

<sup>f</sup>LIDAR Technologies Ltd, Arctic House, Rye Lane, Dunton Green, Sevenoaks,  
Kent, TN145HD, UK, ([mfoster@hovemere.com](mailto:mfoster@hovemere.com))

<sup>g</sup>SensL, Lee House, Riverview Business Park, Bessboro Road, Blackrock, Cork, Ireland,  
([sbellis@sensl.com](mailto:sbellis@sensl.com))

<sup>h</sup>Sula Systems Ltd, Old Crown House, Market Street, Wotton-Under-Edge, GL12 7AE, UK,  
([mhumphries@sula.co.uk](mailto:mhumphries@sula.co.uk))

## ABSTRACT

The European Space Agency (ESA)[1] foresees several robotic missions aimed for the preparation of the future Human Exploration of Mars. To accomplish the mission objectives Imaging LIDARs are one of the identified technologies that shall provide essential information to the spacecraft Guidance, Navigation and Control (GN&C) system. ESA awarded two technology development contracts to two industrial teams for the development and demonstration of novel technologies for Imaging LIDAR sensors. Both teams designed and are manufacturing an Imaging LIDAR breadboard targeting one specific application. The objective of using novel technologies is to reduce substantially the mass and power consumption of Imaging LIDAR sensors. The Imaging LIDAR sensors shall have a mass <10kg, power consumption <60Watt, measure distances up to 5000m, with a field of view (FOV) of 20x20 degrees, range resolutions down to 2 cm, and a frame rate higher than 1 Hz.

**Keywords:** Imaging LIDAR, ESA, GN&C, laser radar, 3D, time of flight, Mars, Moon, rendezvous, landing

## 1. INTRODUCTION

The use of lasers to determine the range of an object from an observer has been utilized in range finding instruments for many years. Many range finding instruments or LIDARs (Light Detection And Ranging) are essentially single beam or 1-dimensional devices in the sense that they determine the distance between the observer and a point on the target. Of particular interest are multidimensional devices which produce an array of such ranges over a specified area of the target and in so doing generate a 3-D image of the target. Such instruments are generally known as Imaging LIDARs.

Imaging LIDARs are considered a key enabling technology for the missions envisaged in ESA's Space Exploration Programme (Aurora Programme)[2]. ESA Aurora Programme foresees several robotic missions where several guidance and navigation tasks require the use of very accurate and high resolution distance measurement systems. To accomplish the mission objectives Imaging LIDARs are one of the identified technologies that have to provide essential information

to the spacecraft Guidance, Navigation and Control (GN&C) systems at important stages of the specific missions, such as entry, descent, landing, rendezvous and docking operations, or robotic surface navigation and exploration operations.

Whereas Imaging LIDAR devices already exist since several years on the commercial market for various metrology and ranging applications, these devices, because of their size, mass and power consumption, are unsuitable for use in planetary exploration missions. Substantial effort is required to achieve technology breakthroughs in order to reduce mass and power consumption of these commercial devices to a level that makes Imaging LIDARs attractive for planetary exploration missions. With these limitations in mind ESA initiated several technology development activities in order to improve current technologies and to develop novel technologies for Imaging LIDAR sensors paving the way for the development of Imaging LIDAR flight hardware. In particular, ESA awarded two contracts under the Technology Research Programme (TRP) [3] to two industrial teams with the objective to develop, demonstrate and validate novel technologies that can improve the performance of Imaging LIDAR sensors and make them suitable instruments for space GN&C applications by reducing their size, mass and power consumption. Within these two activities novel technologies shall be developed and implemented in an Imaging LIDAR breadboard and its performance shall be experimentally demonstrated. After a first phase of the activities where technologies, technical requirements and applications have been reviewed and assessed in detail, the design of a breadboard has been established targeting one application per contract. The manufacturing and testing is currently on going. The team lead by ABSL Space Products (with LIDAR Technologies, SensL and Sula Systems as subcontractors) is developing an Imaging LIDAR breadboard targeting the requirements of the landing application, while the team lead by Jena-Optronik (with RIEGL-Research, Lusospace, Astrium SAS and DLR as subcontractors) is targeting the requirements of the rendezvous and docking application.

## **2. SPACE MISSIONS AND APPLICATIONS**

### **2.1 ESA space missions**

Planetary exploration represents one of the main themes of activity for Europe in space in the coming decades, with missions implemented to the Moon and Mars in the frame of the Aurora Programme. Several key missions are included in this Programme as milestones in terms of development of new technologies, demonstration of key capabilities, and delivering on high priority scientific objectives.

#### **2.1.1 Mars Sample Return (MSR)**

Mars Sample Return (MSR) is one of the flagship missions of the Aurora Programme, not only of Europe, but also of other international partners such as NASA, JAXA etc. Indeed this mission, which aims to return a sample of rocks and soil from the Martian surface back to Earth for detailed analysis, is foreseen to be implemented via a strong international cooperation. Planned sometime in the next decade, the MSR mission involves a complex series of critical operations including a guided entry, descent and soft landing with hazard avoidance, mobile sample acquisition, launch of a Mars Ascent Vehicle (MAV) from the surface into orbit, and an autonomous rendezvous and capture of a small sample container in Mars orbit, before returning the sample to the Earth by means of a high speed Earth re-entry. ESA places a high importance on participation to this landmark mission, and is presently engaged in preparatory activities to ensure a strong participation.

#### **2.1.2 MarsNEXT**

As part of the preparatory activities for MSR, ESA is performing both technology development work, as well as the maturation of PreCursor mission concepts, which aim to demonstrate critical technologies and capabilities required for MSR. One such PreCursor mission is MarsNEXT, planned to be launched within the next decade, the MarsNEXT mission is a combination of both technological and scientific objectives. With the criticality of the rendezvous and capture phase of the MSR mission already highlighted, the MarsNEXT mission will embark a rendezvous and capture experiment to demonstrate the technologies and operations of this key phase. In addition, the mission will embark one of several potential scientific elements, with possibilities ranging from a suite of network science probes, to a single Mars lander, to a dedicated atmospheric analysis package. Each of these options will be studied further in the frame of the exploration programme.

The rendezvous demonstration experiment itself will include a representative sample container dummy which will act as the target for the rendezvous sensors. After acquiring the target at long range with a combination of radio-frequency location system, and camera-based systems, the orbiter will close on the sample container and validate the sensor and GNC performances so critical to the MSR rendezvous phase. Once at close range, the experiment will employ a combination of camera-based navigation sensors and Imaging LIDAR to perform the final closing and terminal approach manoeuvres, up to and including the capture of the sample container via a dedicated mechanism.

### 2.1.3 MoonNEXT

The ESA Aurora Programme recognizes the key role of the Moon in the path of exploration and thus currently studies a Lunar lander mission, also called “MoonNEXT”. This mission, expected to be launched in the next decade, presents an interesting combination of technological, scientific and exploration-preparation objectives, consistent with the broader context of international lunar exploration. The technological objective of MoonNEXT consists in performing autonomously soft precision landing with hazard avoidance on a strongly illuminated site at the Moon’s South Pole (Fig.1). The precision landing capability will be achieved by augmenting the Guidance, Navigation & Control system of the lander vehicle with new-generation sensors and algorithms, which can provide additional information, with respect to the classic use of an Inertial Measurement Unit only. The MoonNEXT soft-precision landing vehicle will typically be equipped with optical cameras, an Imaging LIDAR, or a combination of the two. Based on data coming from these sensors, the on-board navigation computer will perform real-time terrain relative navigation. Advanced and autonomous Hazard Detection and Avoidance (HDA) techniques will also be implemented for MoonNEXT in order to provide the spacecraft with the capability of landing safely on a rough and unpredictable terrain, whilst avoiding hazards, such as slopes, boulders, regions of darkness etc. Data coming from optical sensors already available on-board for navigation is converted to hazard maps, which are then used for safe site identification.

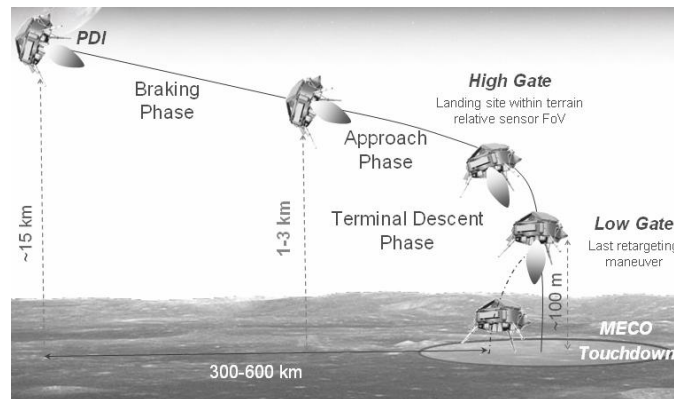


Fig. 1. Typical Lunar decent and landing phase

## 2.2 Imaging LIDAR applications

Imaging LIDAR systems are currently available commercially and used for a wide range of applications including construction site characterization, underwater target recognition, monitoring of mining sites, identification of objects, surface mapping and many others.

However, with some exceptions (the RELAVIS system developed by Optech [4], for example) most currently available systems are unsuitable for space applications because of high mass, large power consumption, poor frame rates or limited range of operation. The recent development of new technologies like novel detector arrays (for example APD arrays), compact scanner systems (for example MOEMs), high power and short pulse laser sources (for example fibre lasers) could lead to the miniaturization of Imaging LIDAR sensors and make them attractive for many space applications such as:

- Controlled soft landing of spacecrafts on planetary bodies
- Navigation and guidance of rovers
- Rendezvous and docking of spacecrafts
- Detection and rendezvous between spacecrafts and asteroids

- Monitoring of large deployable surfaces like antennas, solar panels or airbags
- Optical metrology for spacecraft formation flying
- Examination of spacecrafts external surfaces for integrity verification and damage detection
- Morphological characterization of asteroids

For the landing of a spacecraft on Mars (or Moon), the Imaging LIDAR sensor has to identify safe landing sites on the planet surface during the precisely controlled descent of the landing vehicle. Due to the limited fuel available on the landing vehicle to correct its trajectory, and due to possible high descent velocity ( $>50$  m/s) the Imaging LIDAR sensor has to rapidly scan the planet surface and search for areas that comply with the definition of a safe landing site coping with any residual horizontal velocity. This application requires the operation of the Imaging LIDAR from  $>5000$  m down to 10m, with a FOV of  $20 \times 20$  degrees, an horizontal ground resolution  $<25$ cm at 300m, a range accuracy of 5m (at 5000m) to 2cm (at 10 m) and a frame rate  $> 1$ Hz. The complete system has to have a mass  $<10$  kg and consume less than 60 Watt.

An Imaging LIDAR sensor is expected to support the rendezvous and docking between an orbital spacecraft (Earth re-entry vehicle) and a small orbiting canister coming from the Mars surface with soil samples. The Imaging LIDAR sensor has first to acquire the target at the maximum distance range and then provide target distance and position information to the GN&C system. Then the GN&C system controls the orbital spacecraft attitude and corrects its trajectory to allow its docking with the orbital sample canister. While at long range (from 5000 m to 40 m) the Imaging LIDAR sensor is only required to acquire and track the target, at short distance (typically below 40 m depending on orbiter manoeuvring capabilities) the complete image information of the target will be required for the correct docking and capture operation. This application requires the operation of the Imaging LIDAR from 5000 m down to 1 m, with a FOV of  $20 \times 20$  degrees, an angular resolution better than  $0,1 \times 0,1$  degrees, a range accuracy from 1m (5000 m) to 2cm (at 1 m) and a frame rate  $> 1$ Hz. The complete instrument has to have a mass  $<10$  kg and consume less than 50 Watt. Several cooperative targets are used in the target canister.

### 3. IMAGING LIDAR DEVELOPMENT FOR LANDING APPLICATIONS

#### 3.1 Requirements for the Landing application

After a detailed study of possible landing scenarios, a set of requirements were specified for the breadboard Imaging LIDAR system for planetary landing applications. These requirements are listed in Table 1.

The most difficult requirements are the maximum range of operation, the wide FOV and the high spatial resolution. A comparative analysis of the methods for LIDAR imaging shows that the Time-Of-Fight (TOF) measurement is the only method that could eventually provide the required high performance. However even for this method the solution is not straightforward. A brief evaluation of the range, FOV, and spatial resolution shows that the requirements correspond to an image frame of more than  $1700 \times 1700$  3D pixels, updated every second. Such performance is beyond the capabilities of the traditional TOF scanning systems.

A potential solution is a flash Imaging LIDAR. This is an instrument using a single laser pulse to illuminate the whole FOV and a large array detector to measure TOF in every pixel independently. However, to evaluate the distance to a single pixel from 5km distance one needs some minimum amount of laser power. To measure the whole FOV in the specified conditions in one flash one would require a laser that can produce hundreds of Watts of optical power. This is clearly outside of the allocated mass and power budget.

Table 1. Imaging LIDAR Performance requirements

Maximum range	5000m
Minimum Range	10m
Field of View	$>20^{\circ} \times 20^{\circ}$
Angular/Spatial Resolution	$<0.25\text{m}$ at 300m
Range Accuracy	$<5\text{m}$ (5km); $<0.1\text{m}$ (300m) $<0.02\text{m}$ (10m)
Frame Rate	$>1\text{Hz}$
Vertical landing velocity	50m/s (5000m); $<5\text{m/s}$ (5m)
Horizontal landing velocity	50m/s (5000m); $<5\text{m/s}$ (5m)
Landing vehicle attitude/rate relative to surface	$<2^{\circ}$ / $<0.05^{\circ}/\text{s}$
Safe site landing size	$> 5\text{m} \times 5\text{m}$
Safe local slope / roughness	$<10^{\circ}$ / $<0.5\text{m}$
Azimuth/ Elevation accuracy	$<0.02^{\circ}$
Mass/ Power Consumption	$<10\text{kg}$ / $<60\text{W}$

The optimal solution could be a combination of a detector array and a scanning system. The analysis demonstrated that good performance can be achieved by using a linear array ( $1 \times 256$ ) and a 2D scanning system. Furthermore, evaluation of the spatial resolution requirement led to the selection of a frame of  $1000 \times 1000$  pixels. Such a frame size provides a spatial resolution that is sufficient or better than that required for the proposed GN&C application over all working distances.

### 3.2 Novel imaging LIDAR technologies trade-offs and selection

For any planetary landing system mass and power will be at a premium. Thus if an Imaging LIDAR is to be used for landing on Mars (for example) it is imperative that a solution as compact as possible is chosen. Given the requirements, the Imaging LIDAR must be capable of observing the surface over a distance from 5 km to 10 m with a high level of precision over a large FOV and in a short time scale. This combination of parameters provides significant problems for traditional techniques, such as heterodyne and stereoscopic systems which struggle to cover the complete range of distances. Time-of-flight (TOF) instruments can meet the requirements but tend to be large. This has lead to the development of a TOF system using in the focal plane detector a Silicon photo-diode operating in Geiger mode. The system is highly photon efficient – thus reducing mass while taking advantage of the Time-of-Flight LIDAR flexibility.

### 3.3 Imaging LIDAR breadboard design

#### 3.3.1 Instrument description

The Imaging LIDAR breadboard design is show in Fig 2 and consists of the following elements:

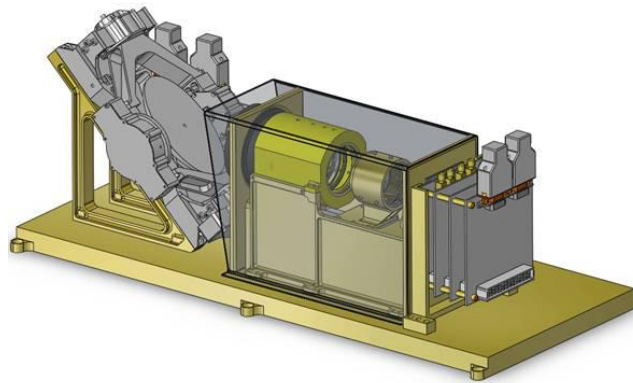


Fig 2. The Imaging LIDAR breadboard.

- **Laser** – emitting short pulses with a repetition rate of 12 kHz at 532nm. The shape of the laser beam is modified to match the FOV of the detector array;
- **Optical system** - comprising of a beam expander, a coupling mirror, a zoom lens and an interference filter;
- **Scanning system** - a single elliptical mirror with two axis of movement. Optical encoders provide information about the position of the mirror;
- **Detector** –  $1 \times 256$  Si SPAD array with custom TOF read-out integrated circuit (ROIC);
- **Control electronics**, including blocks for laser control, motion control, detector control and readout, real time data processing and control, instrument interface and housekeeping and power supply.

The breadboard is constructed of aluminum and designed to be used in laboratory and field test platforms. The current mass of the system is about 8 kg, although the mass of future versions can still be minimized to around 25% less and have a smaller volume package.

### 3.3.2 Optical design

The receiver objective is an especially designed zoom lens made of a single material capable of projecting a high quality image for distances from infinity to one meter. The zoom group is conveniently located in the rear end of the objective, allowing sealing of the whole lens-detector assembly. The input aperture of the lens is 50 mm. This is enough to allow operation from more than 5km. An interference filter with a 1nm bandwidth is positioned in front of the lens to block the background photons.

### 3.3.3 Detector and electronics design

The detector consists of an array of Si Single Photon Avalanche Diodes (SPAD), optimized for fast response and high uniformity at 532 nm. SPADs are attractive with their high sensitivity, established production technology and potential for large array formats. However they have a dead time that is, in principle, too long for this application. One way to circumvent this problem is to exploit the detector capability to respond to the “first” photon. If the detector is used to register to a laser pulse that is shorter than its dead time, it will trigger on the first signal photon and will miss all the other photons in the pulse. A SPAD detector acts as an ideal comparator of a signal level of one photon. At low photon density the trigger event can occur anywhere in the pulse envelope leading to large time measurement uncertainty. However, as the intensity is increased the “first” photon appears closer to the beginning of the pulse and the time uncertainty reduces. This effect can be well described by the theory of probability. It has been proven experimentally that the time uncertainty in response to a ns pulse can be reduced down to tens of picoseconds. Thus by using a SPAD detector in over illumination mode this instrument achieves range resolution better than 20 mm at short ranges.

The electronics consist of several subunits. The main data flow goes through a stack of boards in PC104plus form factor. The key blocks are the detector electronics and Real-Time Data Processing (RTDP) electronics. The detector electronics controls the detector array and formats the TOF data. The RTDP electronics “cleans” and packages the data for transfer to the GNC control computer whilst using a DSP (Digital Signal Processor) and its own memory to extract in real time essential information about spacecraft position and movement.

### 3.3.4 Mechanical and scanner design

The purpose of the scanning system is to extend the FOV from  $5^\circ \times 5^\circ$  to  $20^\circ \times 20^\circ$ . The limited measurement time excludes the use of rotational scanners that generate 2D pseudo-random patterns. Such patterns have variable density and require more laser shots to cover the same area than a regular pattern. For a scanner with regular pattern a linear detector format outperforms a square detector format. Since the scanning system has different energy consumption for  $X$  and  $Y$  axis, its performance can be optimized by selecting a detector format that minimizes the use of the high energy axis.

The selected scanner uses a single elliptical mirror with two axis of movement. It is supported in a gimbal frame and is rotated about its  $X$  axis to provide the horizontal strip scan motion. A second rotation around the  $Y$  axis provides the vertical frame scan motion. The resultant interlaced scan pattern is shown in Fig 3.

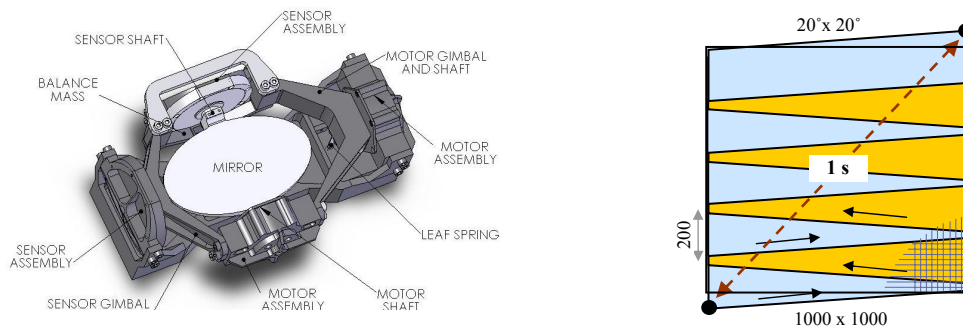


Fig 3. The scan mechanism with assembly (on the left) and the scanning pattern (on the right) .

The scanner operation is decoupled from the transmitter and the receiver and can be independently optimized. The only information needed for RTDP is where it is pointing when the laser is fired. This design flexibility allows minimum power consumption and uniform motion throughout the FOV.

### 3.3.5 Data processing

A feature of the data processing is the use of a Super Resolution Grid (SRG). This concept was especially developed for handling, in real time, the huge amount of data the instrument generates. The SRG is a virtual data container, in which the random spatial points from 3D measurements are assigned to a limited set of possible predefined values. This set has a spatial resolution that is superior to the instrument resolution, hence the name. The SRG houses data from measurements made at different times, allowing for internal data pre-processing. The SRG is referred to the optical axis of the instrument. Its contents can be sent to the GNC computer in a very compact format thus freeing valuable resources that can be concentrated on hazard identification and avoidance.

### 3.3.6 Breadboard operation and performance estimation

The diagram shown in Fig 4 illustrates the operation of the Imaging LIDAR. The instrument consists of several independent functional blocks: laser, optics, detector with specialized TOF ROIC, scanning mirror and control electronics. Additionally, there is a power supply module that is not shown in the diagram. The Real Time Data Processing (RTDP) electronics has also Real-Time Control (RTC) functions, ensuring that the subsystems operate in a synchronized manner. The timing is led by the outgoing laser pulse. The detector measures the moment at which the pulse leaves the instrument and then measures the delay with which the respective pixels register the returned pulse. Once started the scanning mirror moves asynchronously with respect to the laser firing. The motion control electronics guarantees that the mirror moves at fixed X and Y angular rates while pointing inside the instrument FOV. The outgoing pulse is sent to a specific direction into the instrument FOV depending on the position of the mirror. The direction is measured by the XY encoders ("Position data") and later merged with the TOF data.

Since an array detector is used, an image of the object must be projected on the detector. The spatial resolution of the instrument is governed by the size of the detector pixels rather than the laser spot size. As the object moves closer to the target (i.e. the planetary surface), image defocusing occurs. A moving focusing lens group is implemented in the objective to mitigate this issue. The position of this lens group is a function of the distance to the object. An interference filter is used in front of the optical system to block the unwanted background illumination.

In a similar way the RTDP controls the laser intensity so that the detector illumination is kept in an optimum dynamic range. Upon return the laser pulse arrival time is measured on each pixel and the data are sent to the RTDP board. The RTDP merges this data with the position data from mirror encoders and performs some data pre-processing. The data pre-processing extracts the average distance for the purposes of RTC, filters that erroneous measurements and prepares the data in a form convenient for high-speed transfer to GNC over Space Wire interface.

A critical function in the instrument operation is the time gate control. The gate sets the time during which the detector pixels are allowed to see photons. Since the pixels are sensitive to a single photon the instrument needs to "know"



approximately when to open the gate so that only the signal photons are registered. The gate needs to be short enough to block background photons and dark counts but long enough to encompass the target. The RTDP continuously analyses the incoming data using adaptive algorithms to find out where the target is located with respect to the time gate. The RTC then sets the new gate position to keep the target within the gate. The system switches automatically from target tracking to target acquisition if the target is lost.

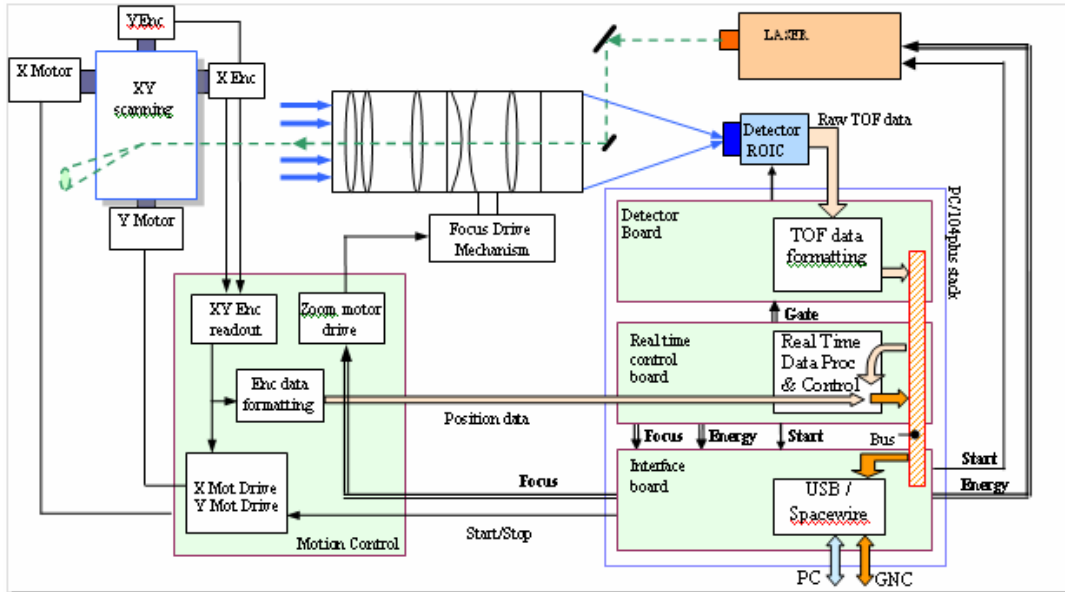


Fig 4. Functional diagram of the Imaging LIDAR.

## 4. IMAGING LIDAR DEVELOPMENT FOR RENDEZVOUZ APPLICATIONS

### 4.1 Requirements for the Landing application

The sensor design is determined by the target's properties and the sensor application conditions including system requirements. The target is defined as a small spherical body of 200 mm diameter that is equipped by retro reflectors (corner cubes) on its surface. It shall be acquired at a range (R) of at least 5 km, and tracked down to  $R=1$  m, before the mechanisms of the orbiter spacecraft will grasp it. A slow but constant tumbling of the sphere is assumed, during its approach to the orbiter spacecraft with a rate of 30 cm/sec down to 1 cm/sec.

The requested 3-sigma range measurement accuracy is as follows:  $\pm 1$  m at  $R = 5$  km;  $\pm 0.55$  m at  $R = 2$  km;  $\pm 0.1$  m at  $R = 150$  m;  $\pm 0.02$  m at  $R = 1$  m. The specified measurement accuracy of Line-of-Sight (LOS) position is 0.2 deg. During target track the update rate of target position determination shall be 1 Hz at least (imaging and subsequent processing of the echo data). The sensor shall be applicable under any Sun incidence condition.

Resulting from target size and minimum range measurement requirement, the total Field of View (FOV) of the sensor is at least 20 deg x 20 deg, reduced size of the scanned area (Field of Regard – FOR) shall be feasible. During track, the FOR shall be resolved by at least 0.05 deg x 0.05 deg. The sensor mass and power consumption shall be minimized, preferably below 7 kg and 45 W for the future space-worthy sensor.

Based on a specification of allowable area coverage and depth of the corner cubes on the target sphere surface, the target definition was refined: corner cube number, arrangement and alignment were optimized in view laser power requirement for long range target acquisition, and of echo power stability for the tumbling sphere. As a result, the target sphere shall be equipped by 12 (dodecahedron) arrays of 6 small corner cubes each.



## 4.2 Novel imaging LIDAR technologies trade-offs and selection

Before starting the sensor design comprehensive trade-offs were performed on method, technology, and component level:

- Between LRF (Laser Range Finder) with collimated beam, combined with beam steering scanners; Flash LIDAR; and Hybrid systems
- Between LRF based on pulsed time-of-flight measurement and phase-measurement
- Between different scanning types and technologies (shape of scan, deflection methods – refractive or reflective, MEMs application, separation of scan axes etc.)
- Between different laser types in the LRF (laser diodes, fiber amplified lasers, solid-state lasers)
- Between different detector types and detection methods in the LRF (APD, PIN diode and arrays hereof or discrete elements; CCDs; Single photon detection etc.)
- Between multi- and single-channel solutions
- Between coaxial and biaxial transmitter/ receiver optics

For the rendezvous concept, the following approaches were selected for the sensor-trade-off since they provide sufficient answers to all design drivers and turned out to be the most promising, based on a feasibility assessment of the necessary technologies, and taking into account the experience of the involved companies:

Concept 1: A scanning LIDAR, based on a single-channel LRF containing diode-laser and Si APD receiver, biaxial transmitter/ receiver optics and separated scan mirrors for azimuth and elevation scan direction.

Concept 2: A scanning LIDAR, based on a single-channel LRF containing fiber laser and InGaAs APD, coaxial transmitter/receiver optics and a gimbal-mounted mirror for azimuth and elevation scan direction.

Concept 3: A scanning LIDAR, based on a single-channel LRF containing fiber laser and InGaAs APD, coaxial transmitter/receiver optics, a MOEM based transmitter beam deflection system combined with a fixed wide iFOV receiver.

Concept 2 was selected out of the 3 concepts, after careful weighting, based on its combination of rather low mass and power consumption. This concept is compliant to frame rate, range domain, and measurement accuracy. It is also insensitivity against Sun incidence and there is high level of maturity development (although with several challenges in view of LRF and Scanner technologies).

## 4.3 Imaging LIDAR breadboard design

### 4.3.1 Instrument description

The following block diagram (Fig. 5) summarizes the sensor modules and their interaction:

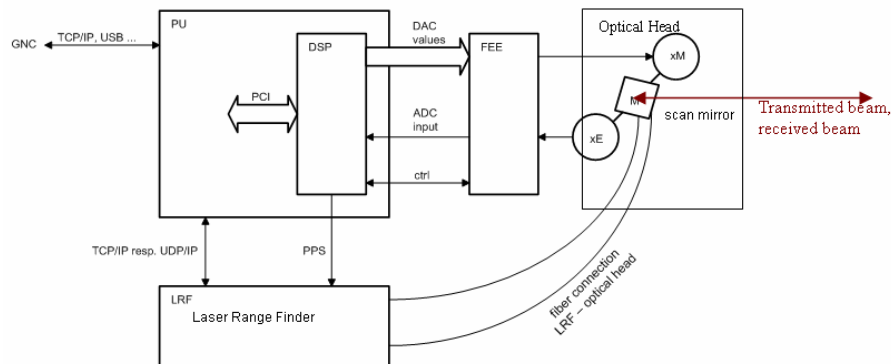


Fig 5. Rendezvous breadboard simplified block diagram

A Fiber Laser inside the LRF sends short laser pulses via a fiber connection to the optical head. The Gimbal-mounted mirror deflects the beam in a mode and range depending on the FOR (within the  $20^\circ \times 20^\circ$  total FOV). The Processor Unit PU serves for coordination of LRF and scanner function, as well as for data assignment and processing. It is

connected with the scanner control electronics through a PCI interface and with the LRF through an Ethernet LAN interface. A PPS interface between scanner control and LRF is implemented to synchronize these units. PU and so the breadboard may be controlled either by means of manual input via the connected peripheral devices (keyboard, mouse, monitor) or by a GNC through a USB 2.0 interface.

#### 4.3.2 Optical, mechanical and scanner design

The optical head (Fig. 6) contains the LRF optics assembly, consisting of a coaxial transmitter and receiver optics, and the scanner head, comprising a Gimbal-mounted scan mirror and the according motors and encoders.

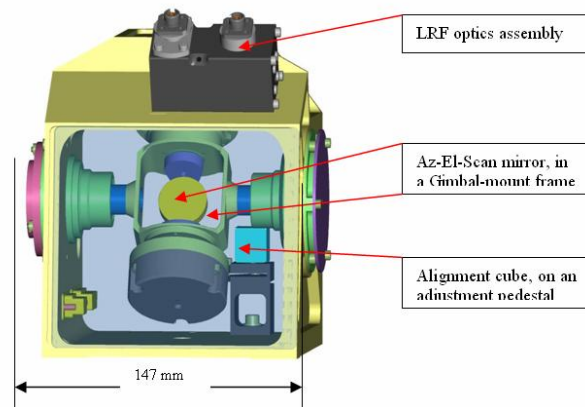


Fig 6. Optical head including LRF and Gimbal mounted scan mechanism

Main attention is paid on a strictly perpendicular evolution of Azimuth and Elevation axes one to each other. The design is driven by the achievable manufacturing accuracy of the component (axes, bearings, Gimbal frame), taking into account the light weighting requirements of the sensor. The scan mirror is made of diamond milled aluminum. This manufacturing technology provides a high flatness and low roughness of the mirror surface, high long-term stability and high reflectivity in the order of  $>95\%$  for the applied laser wavelength of 1550 nm. The rotation point is positioned in the centre of the mirror surface, leading to a fixed origin of the measurement coordinate system independent on mirror deflection.

The coaxial front end consists of laser collimating optics, the receiver focusing optics coupling to an FC fiber port, a beam folding mirror, and the receiver mirror with a center hole for the transmitter beam to pass through (Fig. 7). All components are combined in a stable, compact, and lightweight mechanical structure. This supporting structure comprises several detachable parts and is made of aluminum.

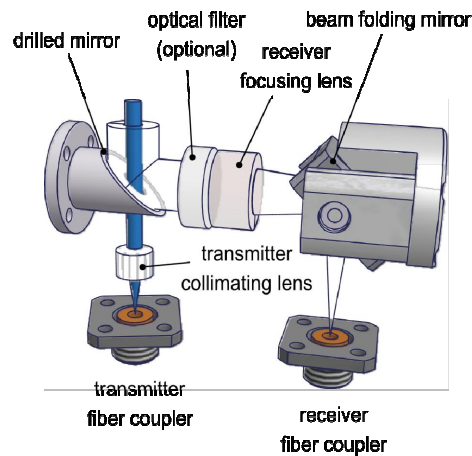


Fig 7. 3D view of the optical front-end.

The tiny transmitter collimator is located at the top. After collimation, the laser beam passes a limiting aperture of 2.5 mm diameter and the center hole of the beam folding mirror of the receiver beam path. This mirror is a diamond-turned copper mirror. In order to minimize optical cross-talk between transmitter channel and receiver channel, the supporting tube of the limiting aperture is extended beyond the mirror surface, but without interfering with the iFOV of the receiver. The receiver beam path after deflection by the beam folding mirror consists of an optional narrow-band filter, a focusing lens mounted in the support structure and another mirror. The receiver fiber coupling may be replaced by directly coupling to a photodiode without any modifications to the optics. The outer dimensions of the optical front-end are 66 mm x 45 mm x 30 mm, the estimated total mass is 150 g.

#### 4.3.3 Detector and electronics design

The LRF is based on pulsed TOF technology with echo digitization. The fiber laser is operated at a pulse repetition rate of 30 kHz, allowing for an unambiguity range of more than 5 km. The pulses are a few nanoseconds wide and echo signals are digitized with sufficient sample rate in order to be able to identify target returns. The receiver frontend comprises an APD with 200  $\mu$ m diameter accompanied by a transimpedance amplifier matched for the signal bandwidth and dynamic range.

The runtime of the echo signal is determined by online waveform analysis of the target returns and reference pulses generated with each laser shot. The device is in principle capable of resolving multiple targets per laser shot, however this is not employed for this application. The range to the target (i.e. the target corresponding to the individual laser shot, generally different to the range to the entire target sphere) is calculated from the runtime, taking into account the signal's group velocity and a system-inherent range offset. The range values are delivered via UDP together with an estimation of the corresponding optical amplitude, time-stamped with an internal clock. Time reference is provided by also delivering the timestamp of the incoming PPS pulses. The LRF also provides a laser trigger (LTR) signal marking the events of outgoing laser pulses for synchronizing with the scanning unit.

#### 4.3.4 Data processing

As a main task, assignment of range and angular measurement is required. The data output consists of a stream of data packages, containing Range, Azimuth, Elevation and Time value for each target return. This output corresponds with a 3-D imaging of the target of up to 30 000 pixels for 1 Hz update rate.

As an alternative for determination of the target centre position (and this is as a basis for precise grasping the target sphere), the image pixels will be processed and evaluated by range depending algorithms, taking into account target motion including tumbling.

#### 4.3.5 Breadboard and performance estimation

For the time being the sensor design and HW (Fig. 8 and Fig. 9) is on elegant breadboard level. The breadboard performance estimation is shown on Table 2.

Table 2. Breadboard performance estimation

Parameter	Performance prediction
FOV	20° x 20°
Frame rate in Track Mode (image update)	1 Hz
Acquisition duration	< 1 min
Min. operational range	<=1m
Max. operational range	>=5000m
Range measurement accuracy 3 $\sigma$ (Sphere centre in TM, by processing of target returns)	5000m > R $\geq$ 2000m: $\Delta R \leq 0.00015 * R + 0.25\text{m}$ 2000m > R $\geq$ 150m: $\Delta R \leq 0.000243 * R + 0.064\text{m}$ 150m > R $\geq$ 10m: $\Delta R \leq 0.000425 * R + 0.0358\text{m}$ 10m > R $\geq$ 1m: $\Delta R \leq 0.00222 * R + 0.0178\text{m}$
Angular measurement accuracy 3 $\sigma$ (Sphere centre in TM, by processing of target returns)	0.2 deg
Laser pulse peak power	200 W
Laser pulse rate	30 kHz

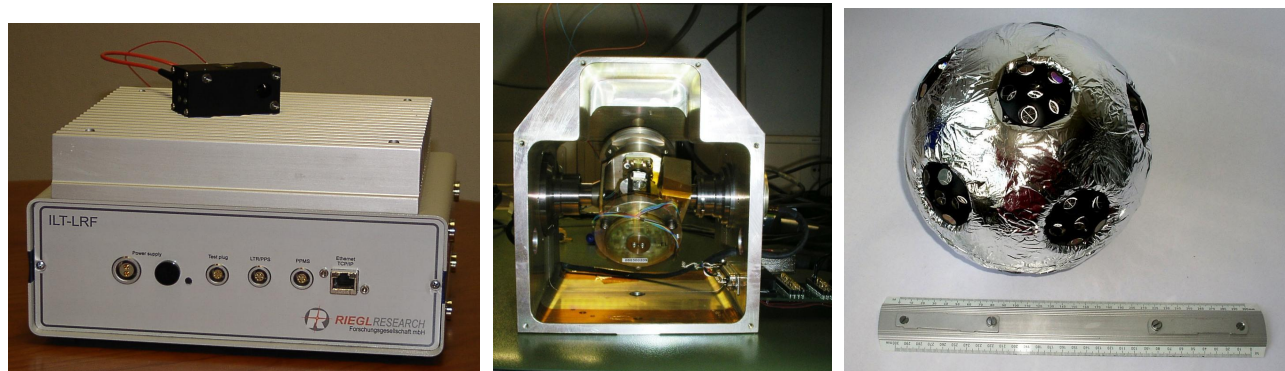


Fig 8. LRF unit and coaxial optical head (left) and the Optical Head (middle) test target sphere (right)

## 5. CONCLUSIONS

Imaging LIDARs are considered a key enabling technology for the missions envisaged in ESA's Aurora Programme where several guidance and navigation tasks require the use of accurate and high resolution imaging and distance measurement systems. Imaging LIDARs are one of the identified technologies that have to provide essential information to the spacecraft GN&C system at important stages of the specific missions, such as entry, descent, landing, rendezvous and docking operations, or robotic surface navigation and exploration operations. With the recent developments on novel laser sources, mechanisms and detectors technologies Imaging LIDARs can overcome the limitations on size, mass and power consumptions that prevented their use in space and several new applications can be envisaged. Two Imaging LIDARs breadboards optimized for two GN&C applications (landing and rendezvous) have been designed and are currently being assembled with several sub-systems completed or near completion. Testing of the system is expected to be performed during last quarter of 2008. Both breadboards implement novel technologies that shall lead to the miniaturization of Imaging LIDAR systems. The breadboards shall provide 3D measurements at long and short ranges (from 1 to 5000m), with large FOVs (20x20 degrees), high spatial and angular resolutions, high distance accuracies (down to 2cm), and shall result in systems with the mass (<10kg) and power consumption (<60W) significantly lower than the initial technical requirements.

## REFERENCES

- [1] European Space Agency; <http://www.esa.int/>
- [2] "Aurora Programme"; <http://www.esa.int/SPECIALS/Aurora/index.html>
- [3] "Imaging LIDAR Technology", ESA Statement of Work, TOS-MMO/2004/797, Issue 1.1, 15<sup>th</sup> February 2005
- [4] J.W.Trip et al; "RELAVIS: the development of a 4-D laser vision system for spacecraft rendezvous and docking operations" presented at Laser Radar Technology And Applications IX 2004 [5412-61]